World Academy of Science, Engineering and Technology
International Journal of Aerospace and Mechanical Engineering
Vol:17, No:10, 2023

Airplane Stability during Climb/Descend Phase Using a Flight Dynamics Simulation

Niloufar Ghoreishi, Ali Nekouzadeh

***Abstract*—**The stability of the flight during maneuvering and in response to probable perturbations is one of the most essential features of an aircraft that should be analyzed and designed for. In this study, we derived the non-linear governing equations of aircraft dynamics during the climb/descend phase and simulated a model aircraft. The corresponding force and moment dimensionless coefficients of the model and their variations with elevator angle and other relevant aerodynamic parameters were measured experimentally. The short-period mode and phugoid mode response were simulated by solving the governing equations numerically and then compared with the desired stability parameters for the particular level, category, and class of the aircraft model. To meet the target stability, a controller was designed and used. This resulted in significant improvement in the stability parameters of the flight.

***Keywords*—**Flight stability, phugoid mode, short period mode, climb phase, damping coefficient.

Glossary of Terms and Symbols

$\vec{\omega} = \begin{bmatrix} p \\ q \\ r \end{bmatrix}_b$	the angular velocity in body coordinate.
$\vec{V} = \begin{bmatrix} U \\ V \\ W \end{bmatrix}_b$	the linear velocity in body coordinate
$\sum \vec{F} = \begin{bmatrix} F_x \\ F_y \\ F_z \end{bmatrix}_b$	total force in body coordinate
$\sum \vec{M} = \begin{bmatrix} L \\ M \\ N \end{bmatrix}_b$	total moment in body coordinate
U_{os}	magnitude of upstream velocity
α	the angle of attack
β	the sideslip angle
φ	the roll angle (or bank angle)
θ	the pitch angle
ψ	the yaw angle
δ_e	the angle of elevator
$\boldsymbol{D}$	the drag force
$\boldsymbol{L}$	the lift force
$\boldsymbol{S}$	the side force
Cx	the dimensionless force coefficient in x direction
Cy	the dimensionless force coefficient in y direction
Cz	the dimensionless force coefficient in z direction
C_l	the dimensionless moment coefficient for L
C_m	the dimensionless moment coefficient for M
C_n	the dimensionless moment coefficient for N

I. Introduction

MOTION of an aircraft and its control is one the most important subjects in design and manufacturing of an aircraft. Multiple approaches and platforms have been developed for analysis of flight dynamics [1]. Flight dynamics generally refers to the six degrees of freedom (d.o.f.) (three linear components and three rotational components) of the aircraft motion in one of the commonly used coordinate systems [1], [2]. The governing equations for these six d.o.f. are nonlinear. Although a rigid body model of aircraft is sufficient for most practical cases, but when the aircraft is very flexible and may undergo significant geometrical changes (other than those intended for flight control), the governing equations of deformation may be included in analysis [2], [3]. For any aircraft, depending on its geometry and velocity, there would be a trim condition where summation of all forces and moments is zero [4]. The nonlinear equations may be linearized about this trim condition for small changes. However, if the nonlinearity is significant and the variations of the aerodynamic properties are not sufficiently small, linearization may result to simulation errors [2], [5]. Flight dynamics may be analyzed for multi airfoil aircrafts and in different flight models [6].

Control of an aircraft is achieved through altering its aerodynamic properties by minor geometrical alterations. These geometrical alterations are usually achieved by three primary controllers: ailerons, elevator, and rudder. Any change in the angle of these controllers' geometries causes the aircraft to transition from one trim condition toward another trim condition. Relations between the position (angle) of these controllers and the aerodynamic properties of the aircraft are required for analysis of flight control and usually determined using scaled models of aircraft with experimental methods [7].

Stability of the aircraft during flight in response to perturbations [8] and changes of the controller angles [9] is one of the most essential features of an aircraft. Rotational stability [8], longitudinal stability [9] and probability of stall [10] are some of the objectives of the stability analysis.

II. Analytical Model

A. Body Coordinate

Body coordinate $\bar{X}_b$ is the coordinate attached to the body of the aircraft with x_b axis along the aircraft cord and y_b along the wingspan, and x-z is the plane of symmetry of the aircraft. Body coordinate is a non-inertial coordinate. In contrast, earth coordinate $\bar{X}_e$ is an inertial coordinate with z_e in the direction of

Niloufar Ghoreishi is with California State University Northridge, CA 91330 USA (corresponding author; e-mail: niloufar.ghoreishi@csun.edu).

Ali Nekouzadeh is with California State University Northridge, CA 91330 USA (e-mail: ali.nekouzadeh@csun.edu).

gravity. Relative position of these two coordinates is defined by three Euler angles: ψ (yaw), θ (pitch) and φ (roll).

$$\bar{X}_b = \begin{bmatrix} 1 & 0 & 0 \\ 0 & \cos\phi & \sin\phi \\ 0 & -\sin\phi & \cos\phi \end{bmatrix} \times \begin{bmatrix} \cos\theta & 0 & -\sin\theta \\ 0 & 1 & 0 \\ \sin\theta & 0 & \cos\theta \end{bmatrix} \times \begin{bmatrix} \cos\psi & \sin\psi & 0 \\ -\sin\psi & \cos\psi & 0 \\ 0 & 0 & 1 \end{bmatrix} \bar{X}_e \quad (1)$$

B. Wind Coordinate

Wind coordinate $\bar{X}_w$ (also called path coordinate) is the coordinate that its *x* axis is along the upstream velocity. Relative position of wind coordinate with respect to body coordinate is defined by two angles: α (angle of attack) and β (sideslip angle).

$$\bar{X}_b = \begin{bmatrix} \cos\alpha & 0 & -\sin\alpha \\ 0 & 1 & 0 \\ \sin\alpha & 0 & \cos\alpha \end{bmatrix} \times \begin{bmatrix} \cos\beta & -\sin\beta & 0 \\ \sin\beta & \cos\beta & 0 \\ 0 & 0 & 1 \end{bmatrix} \bar{X}_w \quad (2)$$

When the sideslip angle is zero, the wind coordinate is called the stability coordinate.

C. Equations of Motion

Body coordinate is a non-inertial coordinate that rotates with respect to the inertial coordinate $\bar{X}_e$. Therefore, the Newton's law of motion of a rigid body in body coordinate may be written as:

$$\sum \vec{F} = m[(\dot{\vec{V}})_b + \vec{\omega} \times \vec{V}] \quad (3)$$

$$\sum \vec{M} = (\dot{\vec{H}})_b + \vec{\omega} \times \vec{H} \quad (4)$$

where $\vec{M}$ is the moment of all forces about the center of gravity, $\vec{H}$ is the angular momentum about the center of gravity, $\vec{\omega}$ is the angular velocity of body coordinate, and $\vec{V}$ is velocity of the center of gravity. If $\boldsymbol{I}$ is the tensor of the moment of inertia in the body coordinate, we may write:

$$(\dot{\vec{H}})_b = I\dot{\vec{\omega}} \quad (5)$$

$$I = \begin{bmatrix} I_{xx} & 0 & -I_{xz} \\ 0 & I_{yy} & 0 \\ -I_{xz} & 0 & I_{zz} \end{bmatrix} \quad (6)$$

Substituting (5) and (6) in (3) and (4), the six governing equations of motion would be:

$$\begin{cases} F_x = m\dot{U} + m(qW - rV) \\ F_y = m\dot{V} + m(rU - pW) \\ F_z = m\dot{W} + m(pV - qU) \end{cases} \quad (7)$$

$$\begin{cases} L = I_{xx}\dot{p} + (I_{zz} - I_{yy})qr - I_{xz}(pq + \dot{r}) \\ M = I_{yy}\dot{q} + (I_{xx} - I_{yy})pr + I_{xz}(p^2 - r^2) \\ N = I_{zz}\dot{r} + (I_{yy} - I_{xx})pq - I_{xz}(\dot{p} - qr) \end{cases} \quad (8)$$

D. Angular Velocity and Euler Angles Rates

Rates of the changes of Euler angles (ψ, θ and φ) determine the angular velocity of the airplane as they define the rotational position of body coordinate with respect to earth inertial coordinate. Based on the definition of Euler angles we may write this relation as:

$$\vec{\omega} = \dot{\phi}\begin{bmatrix} 1 \\ 0 \\ 0 \end{bmatrix} + \dot{\theta}\begin{bmatrix} 1 & 0 & 0 \\ 0 & \cos\phi & \sin\phi \\ 0 & -\sin\phi & \cos\phi \end{bmatrix}\begin{bmatrix} 0 \\ 1 \\ 0 \end{bmatrix} + \dot{\psi}\begin{bmatrix} \cos\theta & 0 & -\sin\theta \\ \sin\phi\sin\theta & \cos\phi & \sin\phi\cos\theta \\ \cos\phi\sin\theta & -\sin\phi & \cos\phi\cos\theta \end{bmatrix}\begin{bmatrix} 0 \\ 0 \\ 1 \end{bmatrix} \quad (9)$$

and the rate of Euler angles can be calculated it terms of angular velocity of the aircraft as:

$$\begin{cases} \dot{\phi} = p + \tan\theta\,(q\sin\phi + r\cos\phi) \\ \dot{\theta} = q\cos\phi - r\sin\phi \\ \dot{\psi} = \frac{q\sin\phi + r\cos\phi}{\cos\theta} \end{cases} \quad (10)$$

Similarly,

$$\vec{\omega} = \dot{\phi}\begin{bmatrix} 1 \\ 0 \\ 0 \end{bmatrix} + \dot{\alpha}\begin{bmatrix} 0 \\ 1 \\ 0 \end{bmatrix} + \dot{\beta}\begin{bmatrix} \cos\theta & 0 & -\sin\theta \\ 0 & 1 & 0 \\ \sin\theta & 0 & \cos\theta \end{bmatrix}\begin{bmatrix} 0 \\ 0 \\ -1 \end{bmatrix} \quad (11)$$

$$\begin{aligned} \dot{\phi} &= p + r\tan\alpha \\ \dot{\alpha} &= q \\ \dot{\beta} &= -r/\cos\alpha \end{aligned} \quad (12)$$

E. Trim Condition and Linearization

At equilibrium, the total force and total moment are zero. Angular velocity and acceleration are zero too. Linear velocity is constant and equal to $\boldsymbol{U}_{so}$, and linear acceleration is zero. We may assume that at equilibrium, velocity is in the aircraft plane of symmetry and airplane does not have any roll angle, meaning that $\varphi = \beta = 0$, $\alpha = \alpha_o$, and $V_o = 0$. Assuming changes in force and moment component are sufficiently small, we may write the linearized form of (7) and (8) for the changes with respect to equilibrium state as:

$$\begin{cases} \Delta F_x = m\Delta\dot{U} + mqW_o \\ \Delta F_y = m\Delta\dot{V} + mrU_o - mpW_o \\ \Delta F_z = m\Delta\dot{W} + mqU_o) \end{cases} \quad (13)$$

$$\begin{cases} \Delta L = I_{xx}\dot{p} - I_{xz}\dot{r} \\ \Delta M = I_{yy}\dot{q} \\ \Delta N = I_{zz}\dot{r} - I_{xz}\dot{p} \end{cases} \quad (14)$$

where $\boldsymbol{U}_o$ and $\boldsymbol{W}_o$ are the components of $\boldsymbol{U}_{so}$ in body coordinate.

To simplify (13) we may transform it to stability (wind) coordinate as:

$$\begin{cases} \Delta F_x = m\Delta\dot{U} \\ \Delta F_y = m\Delta\dot{V} + mr_s U_{os} \\ \Delta F_z = m\Delta\dot{W} + mqU_{os} \end{cases} \quad (15)$$

where r_s is the component of angular velocity r, in stability coordinate:

$$r_s = r\cos\alpha_o - p\sin\alpha_o \quad (16)$$

F. Dimensionless Longitudinal Motion

Dimensionless parameters are defined as:

$$\begin{bmatrix} u \\ v \\ w \end{bmatrix}_b = \frac{1}{U_{os}} \begin{bmatrix} U \\ V \\ W \end{bmatrix}_b \quad (17)$$

$$\begin{bmatrix} \Delta C_x \\ \Delta C_y \\ \Delta C_z \end{bmatrix} = \frac{1}{\frac{1}{2}\rho.U_{os}^2.S} \begin{bmatrix} \Delta F_x \\ \Delta F_y \\ \Delta F_z \end{bmatrix}_b \quad (18)$$

$$\begin{bmatrix} \Delta C_l \\ \Delta C_m \\ \Delta C_n \end{bmatrix} = \begin{bmatrix} 2L/\rho.U_{os}^2.S.b \\ 2M/\rho.U_{os}^2.S.\bar{c} \\ 2N/\rho.U_{os}^2.S.b \end{bmatrix}_b \quad (19)$$

$$m_1 = 2m/\rho U_{os} S \quad (20)$$

$$I_{xx1} = \frac{I_{xx}}{\frac{1}{2}\rho.U_o^2.S.b}; I_{yy1} = \frac{I_{yy}}{\frac{1}{2}\rho.U_o^2.S.\bar{c}}; \\ I_{zz1} = \frac{I_{zz}}{\frac{1}{2}\rho.U_o^2.S.b}; I_{xz1} = \frac{I_{xz}}{\frac{1}{2}\rho.U_o^2.S.b} \quad (21)$$

The dimensionless equations for longitudinal motion with elevator angle as the only input can be written as:

$$\Delta\dot{\theta} = q$$

$$\Delta\dot{\alpha} = \frac{1}{m_1 - C_{z,\dot{\alpha}}c_1}[C_{z,u}u + C_{z,\alpha}\Delta\alpha + (m_1 + C_{z,q}c_1)q + C_{z,\theta}\Delta + C_{z,\delta_e}\Delta\delta_e]$$

$$\dot{q} = \frac{1}{I_{yy1}}[\left(C_{m,u} + \frac{C_{z,u}C_{m,\dot{\alpha}}c_1}{m_1 - C_{z,\dot{\alpha}}c_1}\right)u + \left(C_{m,\alpha} + \frac{C_{z,\alpha}C_{m,\dot{\alpha}}c_1}{m_1 - C_{z,\dot{\alpha}}c_1}\right)\Delta\alpha + \left(C_{m,q}c_1 + \frac{m_1 + C_{z,q}c_1}{m_1 - C_{z,\dot{\alpha}}c_1}C_{m,\dot{\alpha}}c_1\right)q + \left(\frac{C_{z,\theta}C_{m,\dot{\alpha}}c_1}{m_1 - C_{z,\dot{\alpha}}c_1}\right)\Delta\theta + \left(C_{m,\delta_e} + \frac{C_{z,\delta_e}C_{m,\dot{\alpha}}c_1}{m_1 - C_{z,\dot{\alpha}}c_1}\right)]$$

$$\dot{u} = \frac{1}{m_1}[\left(C_{x,u} + \frac{C_{z,u}C_{x,\dot{\alpha}}c_1}{m_1 - C_{z,\dot{\alpha}}c_1}\right)u + \left(C_{x,\alpha} + \frac{C_{z,\alpha}C_{x,\dot{\alpha}}c_1}{m_1 - C_{z,\dot{\alpha}}c_1}\right)\Delta\alpha + \left(C_{x,q}c_1 + \frac{m_1 + C_{z,q}c_1}{m_1 - C_{z,\dot{\alpha}}c_1}C_{x,\dot{\alpha}}c_1\right)q + \left(C_{x,\theta} + \frac{C_{z,\theta}C_{x,\dot{\alpha}}c_1}{m_1 - C_{z,\dot{\alpha}}c_1}\right)\Delta\theta + \left(C_{x,\delta_e} + \frac{C_{z,\delta_e}C_{c,\dot{\alpha}}c_1}{m_1 - C_{z,\dot{\alpha}}c_1}\right)\Delta\delta_e] \quad (22)$$

$$c_1 = \frac{2U_{os}}{\bar{c}} \text{ and } c_2 = \frac{2U_{os}}{b}.$$

which can be written in state space as:

$$\dot{\underline{X}} = A\underline{X} + B\Delta\delta_e \quad (23)$$

$$\underline{X} = \begin{bmatrix} U \\ \Delta\alpha \\ q \\ \Delta\theta \end{bmatrix} \quad (24)$$

$$q = \Delta\dot{\theta}$$

III. Simulation Results

A. Aircraft Performance Simulation

Elements of matrix **A** and vector **B** were calculated based on the existing measurements of the dimensionless coefficients of force and moment, and their variations by state variables and elevator angle about the equilibrium condition at U_{os} = 53.77 m/s and $\theta_o = 0$.

$$A = \begin{bmatrix} -0.044 & 0.035 & 0 & -0.181 \\ -0.362 & 1.983 & 0.973 & 0 \\ 0.323 & -6.872 & -2.902 & 0 \\ 0 & 0 & 1 & 0 \end{bmatrix}$$

$$B = \begin{bmatrix} 0 \\ -0.158 \\ -11.535 \\ 0 \end{bmatrix}$$

The resultant characteristic equation has two pairs of complex conjugate poles:

$$P_{1,2} = -2.448 \pm 2.453\mathbf{i}$$

$$P_{3,4} = -0.0165 \pm 0.2126\mathbf{i}$$

The first pair defines the short period mode with natural frequency and damping ratio of:

$$\omega_{ns} = 3.530$$

$$\zeta_s = 0.6935$$

The second pair defines the phugoid mode with natural frequency and damping ration of:

$$\omega_{np} = 0.213$$

$$\zeta_p = 0.0774$$

The governing equations of motion were solved numerically for a 1° step change in the elevator angle using MATLAB. The solutions for state variables are shown in Figs. 1-8 in two timescales. The short period mode solutions are shown in a fine time scale (0-4s) and the phugoid modes are shown in a courser time scale (0-400s).

In response to the 1° change in the elevator angle, velocity U starts to increase from its initial equilibrium magnitude of 53.77 m/s (Fig. 1).

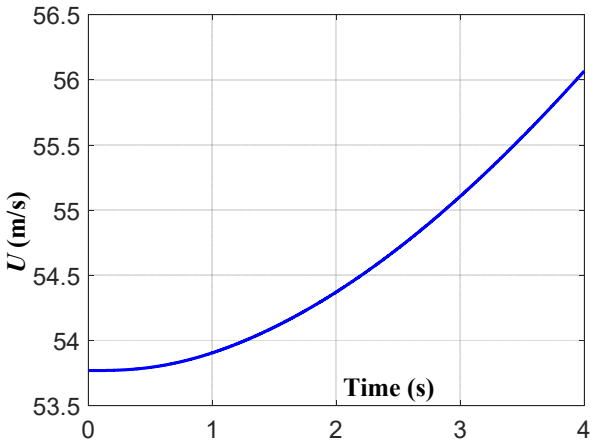

Fig. 1 Aircraft velocity in short period mode in response to 1° increase in elevator angle

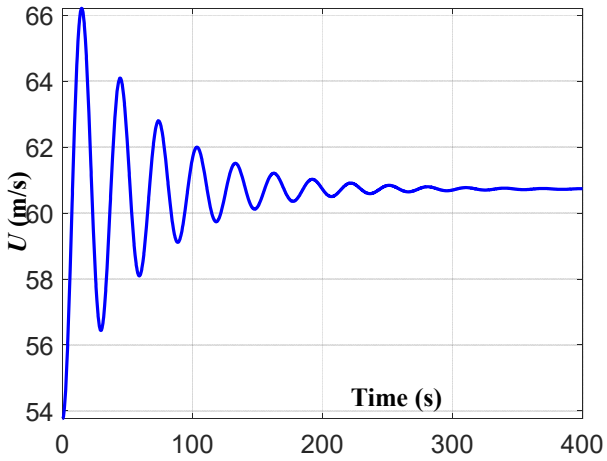

Fig. 2 Aircraft velocity in phugoid mode in response to 1° increase in elevator angle

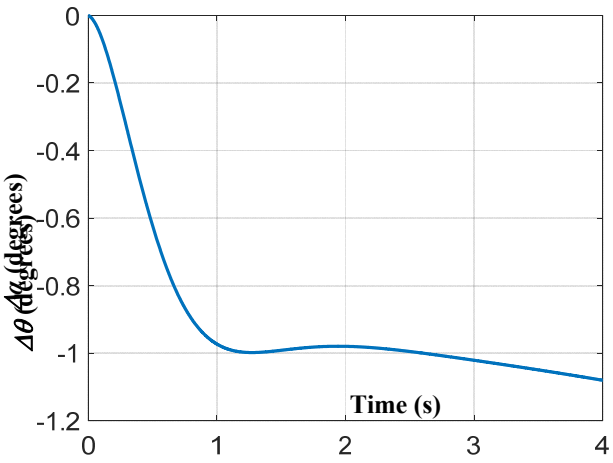

Fig. 3 Changes of the angle of attack, $\Delta\alpha$, in short period mode in response to 1° increase in elevator angle

Velocity continues to rise to a maximum of 66.21 m/s and approaches to final value of 60.74 m/s in an oscillatory form (underdamp response) in phugoid mode (Fig. 2). Velocity response has a maximum overshoot of 78.5%.

The angle of attack drops by about 1° within 1 second of the change in elevator angle in the short period mode (Fig. 3) and continues to drop more gradually and in an oscillatory form in phugoid mode (Fig. 4). Change of the angle of attack approaches a final value of -1.35° and passes through a maximum change of -1.68° (max overshoot of 24.1% overshoot). Note that as the elevator angle is increased the aircraft experiences a descend.

Increasing the elevator angle causes a downward angular velocity for the aircraft ($q < 0$) which results to reduction of pitch angle, θ.

The angular velocity increases (in negative direction) to -2.4 degree/s within 0.5 s and then starts to return to zero in short period mode (Fig. 5). Over time and in phugoid mode, the angular velocity approaches zero at the new equilibrium state of the aircraft (Fig. 6). This angular velocity varies in both positive and negative directions, causing the pitch angle to increase and decrease (oscillation of airplane).

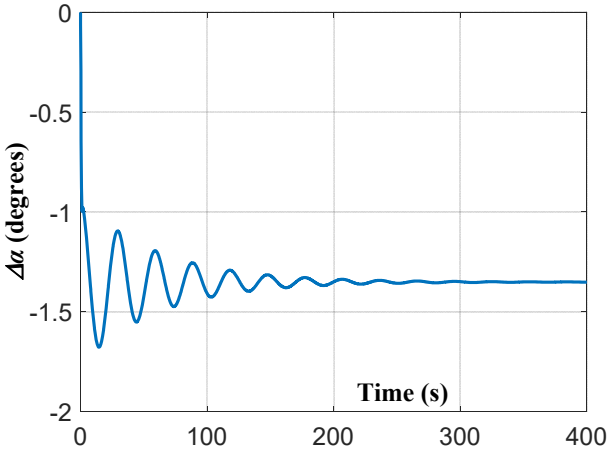

Fig. 4 Changes of the angle of attack, $\Delta\alpha$, in phugoid mode in response to 1° increase in elevator angle

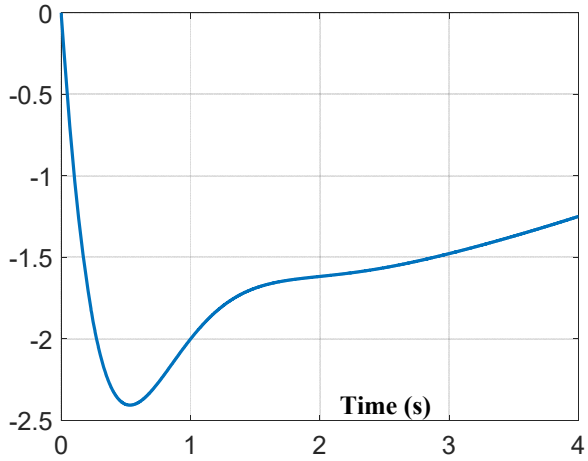

Fig. 5 Angular velocity q (of the pitch angle), in short period mode in response to 1° increase in elevator angle

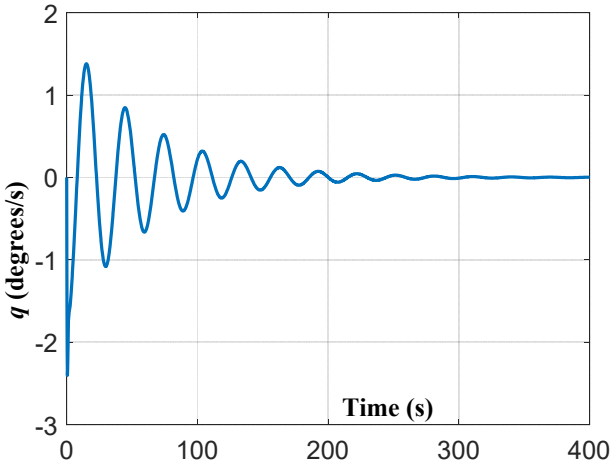

Fig. 6 Angular velocity q (of the pitch angle), in phugoid mode in response to 1° increase in elevator angle

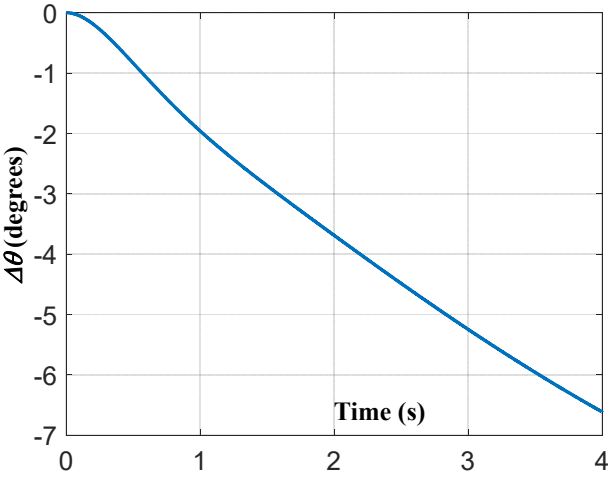

Fig. 7 Changes of pitch angle $\Delta\theta$, in phugoid mode in response to 1° increase in elevator angle

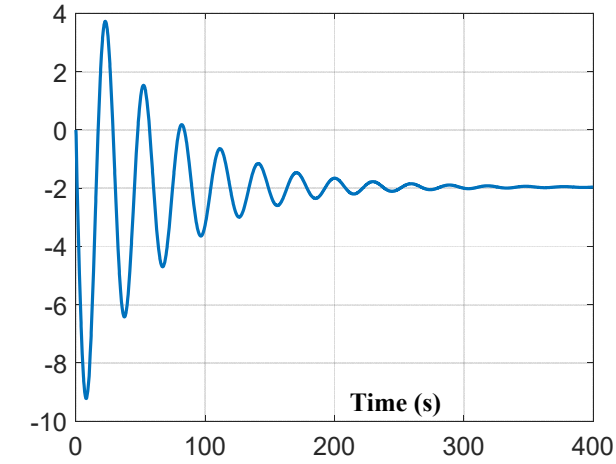

Fig. 8 Changes of pitch angle $\Delta\theta$, in phugoid mode in response to 1° increase in elevator angle

Pitch angle reduces quickly and continuously by several degrees in short period mode (Fig. 7). After about 8s the change of pitch angle is about -9.2°. In phugoid mode the pitch angle oscillates with a relatively large amplitude toward a final change of -1.97° for the new equilibrium state. Airplane experiences a maximum overshoot of about 370% in the pitch angle during the transition to the new equilibrium state. This indicated that the amplitude of the oscillations in pitch angle is excessive.

The damping frequency of this motion is ω_d = 0.21 rad/s. This is the frequency of the oscillations of the pitch angle in phugoid mode.

B. Desired Performance

This aircraft is considered *Level I* (should have adequate flying qualities for its mission), *Category A* (non-terminal flight phase that requires rapid maneuvering and precise tracking), and *Class I* (small light airplane). Based on these classifications this aircraft should have a natural frequency of about ω_n = 0.2 rad/s and damping ratio of about ζ = 0.2 in phugoid mode, and a natural frequency of about ω_n = 5.26 rad/s and damping ratio of about ζ = 0.91 in short period mode.

Comparing the natural frequencies of this aircraft with these desired values, the short period mode is close to the desired performance, but the phugoid mode has a damping coefficient that is three times smaller than the desired value, and as the results is significantly more underdamped than allowed.

The performance of the airplane can be improved by changing the design of its geometry or by adding a controller mechanism. In the following section we show how we were able to improve the performance of this aircraft by a PID controller.

C. Improvement of Performance

To improve the performance of this aircraft, a PID controller was used. This controller uses a feedback signal from the pitch angle, θ, to optimize the input signal (δ_e, the angle of elevator). The diagram of this PID controller is shown in Fig. 9. This controller is intended to improve the transient response of $\Delta\theta$ angle. The reference signal is intended to set (control) the steady state value of pitch angle, θ.

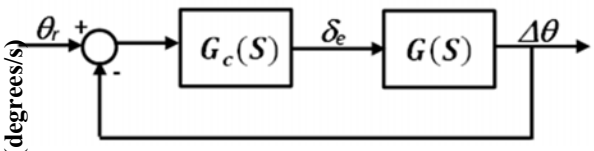

Fig. 9 Schematic of the PID controller used to improve the transient response of the flight and in particular the pitch angle.

Using pole placement technique, the PID controller was designed as:

$$G_c(S) = -0.16\frac{(S+0.11)^2}{s} \quad (25)$$

The resultant closed loop system has the following poles:

$$P_{1,2} = -3.345 \pm 2.202\mathbf{i}$$

$$P_{3,4} = -0.0404 \pm 0.196\mathbf{i}$$

$$P_5 = -0.003$$

The additional real pole is very close to origin and settles slowly. It does not have any impact on short period mode. The first pair of poles defines the short period mode with natural frequency and damping ratio of:

$$\omega_{ns} = 4.005$$

$$\zeta_s = 0.835$$

The second pair of poles defines the phugoid mode with natural frequency and damping ratio of:

$$\omega_{np} = 0.200$$

$$\zeta_p = 0.201$$

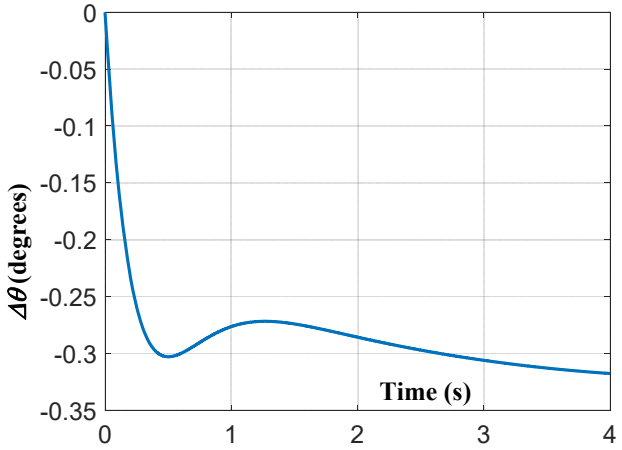

Fig. 10 Changes of pitch angle $\Delta\theta$, in short period mode in response to 1° decrease of pitch angle reference input with the PID controller

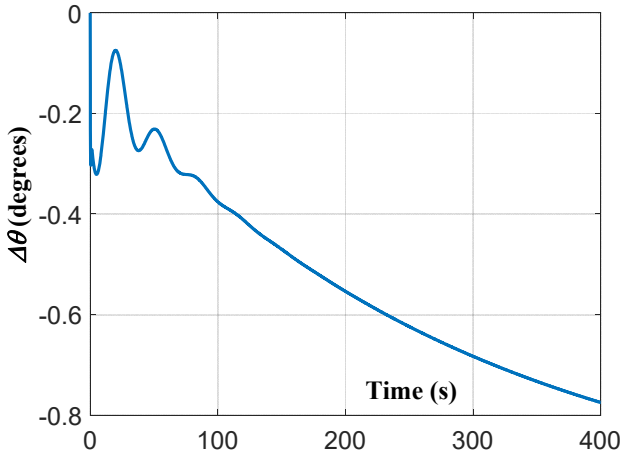

Fig. 11 Changes of pitch angle $\Delta\theta$, in phugoid mode in response to 1° decrease of pitch angle reference input with the PID controller

The designed PID controller enables the aircraft to meet the target performance of phugoid mode and improves the performance of short period mode. The closed loop control system was used to simulate the transient response of the pitch angle to a unit step change in pitch angle reference input. The simulated pitch angle with the improved flight control system is shown in Fig. 10 for short period mode and in Fig. 11 for phugoid mode. These figures are the variation of pitch angle in response to 1° step reduction of pitch angle reference input. For this input in the pitch angle reference input, the resultant steady state change in elevator angle is about 0.5° increase.

Adding the PID controller reduced the underdamp and oscillatory behavior of the response and there is no overshoot in the response anymore. However, the overall response time is increased (due to additional added real pole) and the response that was settled at about 300 s in aircraft without a controller is far from settling at 400 s when the PID controller is added.

IV. Conclusion

Governing equations of flight dynamics were derived for longitudinal motion of an aircraft in climb/descend phase. Using the experimentally determined force and moment dimensionless coefficients and their variations with aerodynamic properties and elevator angle of a model aircraft, the dynamics and stability in climb/descend longitudinal motion was simulated numerically.

As the model aircraft was away from the desired stability parameters in phugoid mode (excessive underdamp response), a PID controller was used to improve its stability. PID controller improved the stability of the aircraft to meet its target values, but the improvement came at the cost of increasing the response time (settling time) of the aircraft.

Acknowledgment

Authors are greatly thankful to Dr. Kenneth Jerina for providing the force and moment coefficients of the aircraft model and defining the objectives of this project.

References

[1] W. Durham, "Aircraft Flight Dynamics and Control," John Wiley and Sons, Ed. 1, 2013.

[2] M. Shearer and C. E. S. Cesnik, "Nonlinear Flight Dynamics of Very Flexible Aircraft," *Journal of Aircraft*, vol. 44, no. 5, pp. 1528–1545. 2007.

[3] J. M. Dietl and E. Garcia, "Stability in Ornithopter Longitudinal Flight Dynamics," *Journal of Guidance, Control, and Dynamics,* vol. 31, no. 4, pp. 1157–1163, 2008.

[4] D. Pucci, "On the Existence of Flight Equilibria in Longitudinal Dynamics," *2019 IEEE 58th Conference on Decision and Control (CDC)*, pp. 5894-5899, 2019.

[5] D. H. Nguyen, M. H. Lowenberg and S. A. Neild, "Frequency-Domain Bifurcation Analysis of a Nonlinear Flight Dynamics Model," *Journal of Guidance, Control, and Dynamics*, vol. 44, no. 1, pp. 138–15, 2021.

[6] C. Montalvo and M. Costello, "Meta Aircraft Flight Dynamics," *Journal of Aircraft*, vol. 52, no. 1, pp. 107–115, 2015.

[7] B. Owens, J. Brandon, M. Croom, M. Fremaux, G. Heim and D. Vicroy, "Overview of Dynamic Test Techniques for Flight Dynamics Research at NASA LaRC," *25 AIAA Conference on Aerodynamic Measurement Technology and Ground Testing*, San Francisco CA, AIAA Paper 2011-3504, 5-8 June 2006.

[8] N. Nguyen, K. Krishnakumar, J. Kaneshige and P. Nespeca, "Flight Dynamics and Hybrid Adaptive Control of Damaged Aircraft," *Journal of Guidance, Control, and Dynamics*0, vol. 31, no. 3, pp. 751–764, 2008.

[9] F. Gavilan, J. Á. Acosta, R. Vazquez, "Control of the longitudinal flight

dynamics of an UAV using adaptive backstepping," *IFAC Proceedings Volumes*, vol. 44, no. 1, pp. 1892-1897, January 2011.

[10] D. Pucci, "Flight dynamics and control in relation to stall," *2012 American Control Conference (ACC)*, Montreal QC Canada, pp. 118-124, 27-29 June 2012.